STUDY ON MASS COMPOSITION OF EXTENSIVE AIR SHOWER WITH ULTRA HIGH ENERGY COSMIC RAYS USING Q PARAMETER AND THEIR MUON COMPONENT

Maryam MORADALIZADEH[1], Saeed DOOSTMOHAMMADI[1*], Jalil FATEMI[1], Hamid ARJOMAND KERMANI[1]

Mass Composition (MC) of Cosmic Rays at high energies is one of the most important issues which are significantly related to astrophysical sources. At present work, we have tried to study the spatial parameters, such as age parameter, slope of lateral distribution function of electrons, and muon density of air shower. Each parameter will be discussed separately and also their effect on MC of cosmic rays with energy above 10^{18}eV will be considered. The Yakutsk Extensive Air Shower array data was used in our work. Moreover, the present results can be used to distinguish the popular top-down and bottom-up models of astrophysical sources of high energy cosmic rays.

Keywords: Cosmic Ray, Age Parameter, Lateral Distribution Function. Muon component.

1. Introduction

Cosmic Rays (CR) are high energy charged particles or photons that are produced in various astrophysical sources and detected on the earth surface. The particles that have energy above 10^{18} eV are known as ultra-high energy CR.The sources of these particles and their acceleration mechanisms are still unknown. Studying these particles and their sources is very important and can provide valuable information about cosmic accelerator toward understanding the universe.

When a CR particle with enough energy hits the Earth's atmosphere, a cascade of secondary particles will be produced which is called Extensive Air Shower (EAS). A large number of array detectors in fix distance at ground surface are being used to record these secondary particles. When the primary CR energy increases, the number of generated secondary particles increases as well. Large Arrays are used to increase the chances of recording of the secondary particles, because high energy particles have very low flux so the low flux should be compensated by increasing the area of detector arrays.

Depending on which of two theoretical models is used, the set of astrophysical sources is different. The first one is the top-down model with a non-

[1] Department of Physics, S. B. University of Kerman, Iran, email: doostmohammadis@gmail.com

accelerated approach (fission) and the second one is the bottom-up model with an acceleration approach.

With different interpretations, there are conflicting results in fractions of primary photons and their astrophysical sources in high-energy levels from the experimental point of view. For example, AGASA Group suggests a high fraction in primary photons that confirms the top-down model [1]. On the one hand the Auger detector group disagrees with this assertion [2].

On the other hand, the portion of photons with energies above 10^{19} eV suggested by Auger group is about 8.9 percent [3]. High portions 50% of the predicted photons of the CRs in high-energy levels are used to describe the sources of CRs with the top-down model. However, severe restrictions have been applied on these models by previous studies on photons with energies over 10^{19} eV [4]. While, in bottom-up model the amount is very low the order is less than 0.1% [5].

In addition, it is expected that smaller share of photons for instance 0.01to1% in energies above 10^{19} eV [6] are produced During the photo-pion production processes by the collision of CRs with the cosmic microwave background [7, 8].

Pierre Auger Observatory has presented a decrease in the flux of CRs in the energy range above 10^{19} eV [9, 10] which is compatible with the prediction of GZK cutoff, and also this flux reduction of CRs in the spectrum can be related to photon disintegration. The comparability of the observation of photon flux with the predictions of the theory can independently prove the phenomenon of GZK cutoff.

By the hybrid detectors of Pierre Auger Observatory, an upper limit of photon fractions for energies above 10^{19} eV has been extended [11]. In the present work, the data of Yakutsk array detector [12] with an area of 18 square kilometers near Yakutsk in Russia (latitude 62 north and longitude 129 east) which is located at an altitude of 105 meters above sea level equivalent to the atmospheric 1020 g/cm^2 have been used in order to obtain the percentage composition of the primary CRs that have energies above 5×10^{18} eV.

This data includes 36 EASs, each of which has a density of electron and muon in versus distance from the shower core which primary energy, zenith angle θ, location and Moliere radius for each shower is recorded. Their energy range vary between 5×10^{18} eV to 7×10^{19} eV and their zenith angle is something about 0 to 60^o. To determine the composition of CRs with energy range above 5×10^{18} eV some sensitive parameters to MCs have been considered.

2. Observables related to mass separation

2.1. Q Parameter

As mentioned, in order to investigate the composition of CRs at high energy, a parameter called Q is defined as follows:

$$Q(R)=\frac{\rho(400)-\rho(R)}{\rho(400)} \qquad (1)$$

In which $\rho(400)$ is the electron density at distance of 400 meters from the shower core, and similarly $\rho(R)$ is the electron density at R distance (more than 400 meters) from the core.

In this study, it has been tried to use the Q parameter to compare the broadness distribution of electron density around the shower core. As the Q value for any specific shower where distance from the core was greater, the concentrating densities around the core became higher. In other words, it demonstrates the electron density focus around the shower center. Fig. 1 and Fig. 2 illustrates the value of Q parameter diagram versus R for primary particle with different MC. Whatever the Q parameter increase, MC of primary particles goes toward lighter nucleus.

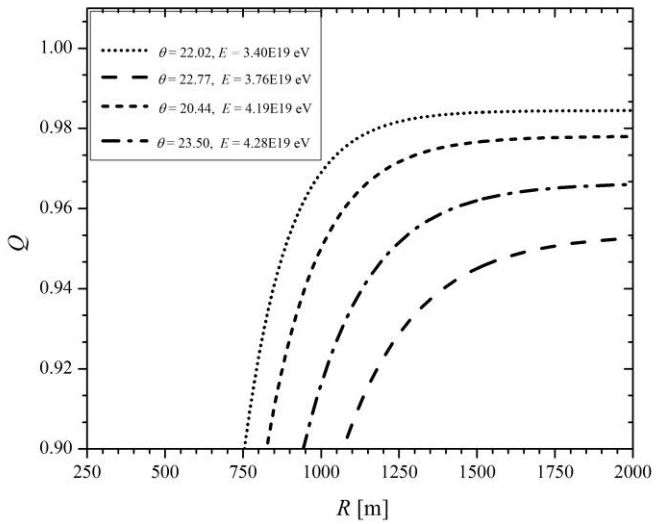

Fig. 1. The variation of Q vs. R for four registered EAS of Yakutsk array.

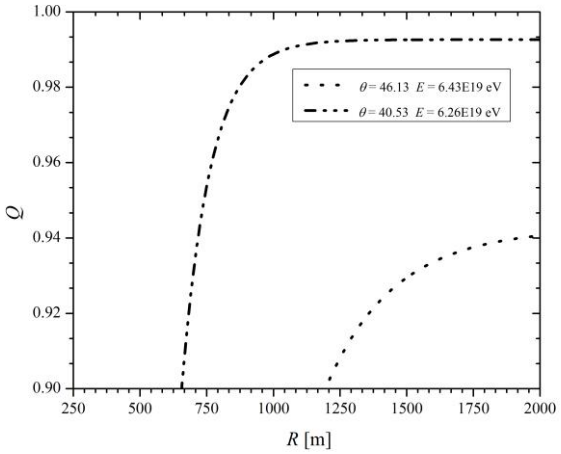

Fig. 2. The variations of Q vs. R for two registered EAS of Yakutsk array.

Thus, at the moment, the Q parameter was used as one of the parameters that are sensitive to MC within the core distances from 600 m to 2000 m. Since the results of this parameter is achieved by two density proportions, the dependency of this parameter to primary energy and also zenith angle will be removed. Furthermore, the Q parameter versus primary energy at the distances of 600 m and also 2000 m from the core was plotted. According to these diagrams it is obvious that by increasing primary energy, the value of Q parameter is increased in energy above about 9×10^{18} eV. This means that the MC will be decreased in this energy range. Another variation is related to energies above 3.4×10^{19}eV. Also a decrease in the Q parameter is seen at the energy above 3.4×10^{19}eV which indicates an increase in MC of primary CRs at this energy range. See Fig. 3. and Fig. 4. Here we can say the fact that Q parameter does not depend directly on energy, even if it is a ratio, is still a hypothesis.

As expected, an evidence for MC increasing at energies above 3.4×10^{19}eV is seen, this effect is more announced at larger distance of shower core (i.e. 2000 m) as shown in Fig. 4.

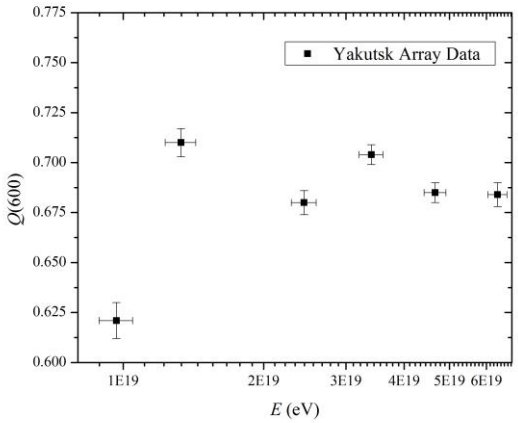

Fig. 3. The variations of Q (600) vs. energy

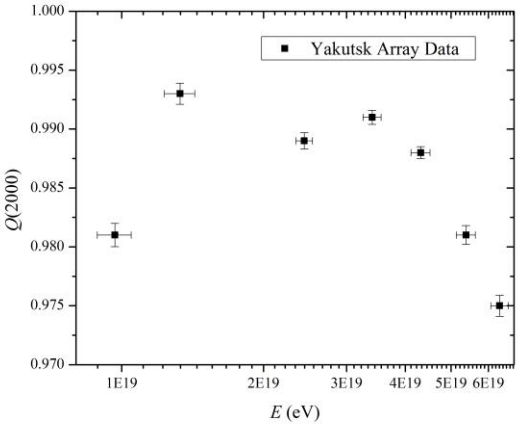

Fig. 4. The variations of Q (2000) vs. energy

2. 2. Age parameter S

One of the most important parameters in the study of MC of the EASs is its s. Since the maximum depth depends on the initial shower energy and particle mass, this feature can be used to determine the MC [13]. S quantity is a sensitive parameter to the MC that are described by the theory of electromagnetic cascade [14]. This theory predicts that the shower S decreases with increasing energy. But if the MC of elementary particles changes (such as protons to iron nuclei), the S increases with increasing energy. The Increase of S with the increase of MC has been recently shown by other researchers [15].

In addition, the increases of the MC for energies above (3 - 4) $\times 10^{19}$ eV by increase of S at this energy have been suggested by our previous work [16]. In

this study, to get the S, electron density diagram versus core distance was plotted for each shower. Then the fitting of Nishimura-Kamata-Greisen function on the electron density versus core distance were performed, and S and shower size N_e are obtained for each shower [17,18].

$$\rho_e(r)=\frac{N_e}{r_0^2}F\left(\frac{r}{r_0}\right) \qquad (2)$$

where $\rho_e(r)$ is the electron density at the core distance of r (in r_0 unit) and N_e is the shower size and

$$F\left(\frac{r}{r_0}\right)=c(s)\left(\frac{r}{r_0}\right)^{s-2}\left(1+\frac{r}{r_0}\right)^{s-4.5} \qquad (3)$$

where S is the shower age, c(s) is a function of s, and r_0 is the Moliere unit. After obtaining the S for showers in order to elucidate the dependence of S to zenith angle S graph versus zenith angle was plotted. This graph shows the increase dependency of S with zenith angles θ. The increase was 0.04 per 10^o zenith angle range.

2.3. The slope of the lateral electron density distribution function β.

Another parameter used to separate MC of CRs is electron density lateral distribution function slope β. The absolute value of the slope for the heavier particles such as iron is low and for the lighter particles such as proton and gamma will be increased.

In order to obtain the slope of the lateral electron density distribution versus core distances of the shower, the relationship (2) and (3) were used, and then the slope of the fitted line through the corresponding points is calculated. Different electron density lateral distribution function slope for primary particles with different MC have been shown in Fig. 5. and Fig. 6.

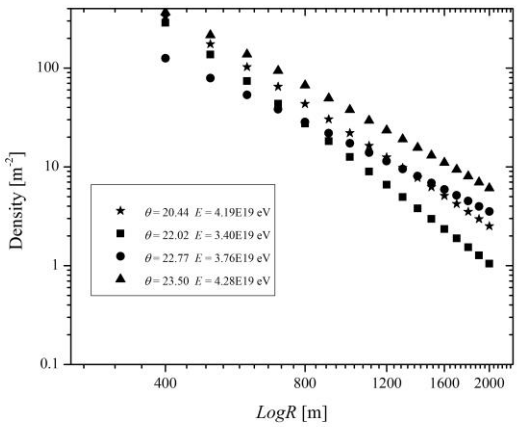

Fig. 5. The lateral distribution function of electron (LDF) for four different particle types, the showers are detected by Yakutsk array, each slope is measured from the fitted lines in the figure.

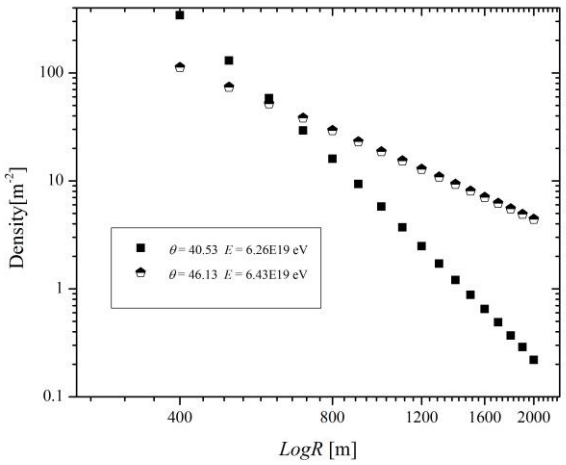

Fig. 6. The lateral distribution function of electron (LDF) for two different particle types, the showers are detected by Yakutsk array, each slope is measured from the fitted lines in the figure.

After obtaining the parameter β for showers to elucidate dependency of β parameter on the zenith angle, the graph of β parameter versus zenith angles was plotted. This graph shows the increase dependency of β parameter on the shower zenith angle. The β increase was 0.06 per 10^o of zenith angles. However, βparameter sensibility to MC has been clearly shown in Fig. 7.

One can see the variation of MC of high energies by using the slope of electron lateral distribution β vs. primary energy. Regarding to Fig. 7. two examples of slopes are seen. The First example, which is shows the increase of

slope in energy above 8.5 $\times 10^{18}$ eV, is related to the decrease in MC. Also, the second example, which is due to the decrease of electron lateral distribution function slope of shower in energy above 4.3 $\times 10^{19}$ eV, is related to the increase of MC at this energy range. Therefore, regarding to this diagram, it is expected that MC of elements is increased at energies above 4.3 $\times 10^{19}$ eV.

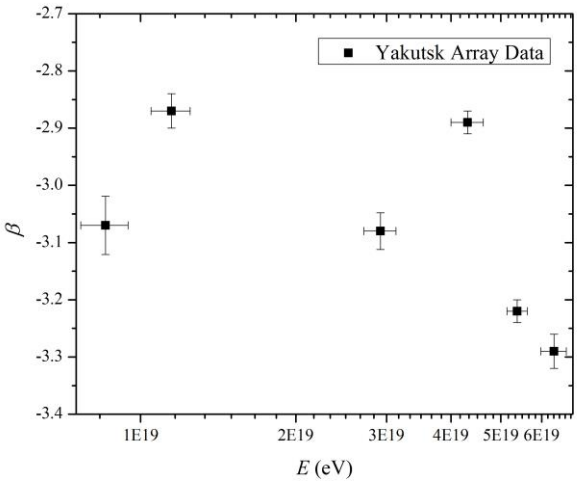

Fig. 7. Electron Lateral Distribution Function slope vs. Energy of Primary EAS

2.4. Muon component of EAS

Muon component of EAS is one of the important, sensitive and qualitative parameters to MC of CRs in high energies. Since, in the heavy particle spallation, the nucleons are generated more in comparison with lighter particles such as proton and even gamma, the heavy particles produce much more muons than lighter ones. At the present work, muon density at distance of 1000 m from the core is calculated by using Yakutsk array data and the assumption of Hayashida and Greisen formula [19].

Hayashida formula:

$$\rho_\mu(r) = N_\mu \left(\frac{c_\mu}{R_0^{\,2}}\right) r^{-\alpha} (1+r)^{-\beta} \left[1+\left(\frac{R}{800}\right)^3\right]^{-\delta} \qquad (4)$$

Where $r = \frac{R}{R_0}$ (R is core distance), $c_\mu =$ 0.262 (for R < 800 meters), $c_\mu = 0.325$ (for R > 800 meters), $\beta =$ 2.52, $\delta =$ 0.6, $\alpha =$ 0.75, $R_o =$ 0.66 (for secθ < 1.1) and $\text{Log}(R_o) = 0.58\,(\sec\theta - 1) + 2.39$ (for 1.1 < secθ < 1.8).

Greisen formula: (for secθ < 1.2 and R < 800 meters).

$$\rho_\mu = N_\mu \left(\frac{c_\mu}{R_0^{\,2}} \right) r^{-\alpha} (1+r)^{-\beta} \qquad (5)$$

which N_μ is obtained as follow:

$$N_\mu = (2.6 \pm 1.4) \times 10^{a+5} \left(\frac{N_e}{10^7} \right)^b \text{; in which}$$

$$a = (1.07 \pm 0.13)(sec\theta - 1), b = (0.77 \pm 0.02) - (0.17 \pm 0.02)(sec\theta - 1) \qquad (6)$$

The following equation is used for sec ≥ 1.2 as well:

$$Log\left(\frac{\rho_\mu(600)}{S(600)}\right) = ALogS(600) + B \qquad (7)$$

S(600) is electron density at distance of 600 m from the core and A,B is the constant defined from Table 1.

Table 1.

A and B constants

$Sec\theta$	A	B
1.2 - 1.4	-0.16 ± 0.01	-0.58 ± 0.01
1.4 - 1.6	-0.17 ± 0.04	-0.40 ± 0.02
1.6 - 1.8	-0.22 ± 0.10	-0.30 ± 0.03
1.8 - 2	-0.30 ± 0.22	-0.21 ± 0.06

After calculating $\rho_\mu(600)$, by using relationship of (7), the value of $\rho_\mu(600)$ is substituted in Greisen formula and then $\rho_\mu(1000)$ is obtained. Then muon data were analyzed and two considerable variations in energies about 9.96 $\times 10^{18}$ eV and also 3.48 $\times 10^{19}$ eV are seen in the diagram of $\rho_\mu(1000)$ and $\rho_\mu(600)$ vs. energy. These variations indicate a decrease and an increase in muon size of EAS in energies of 9.96 $\times 10^{18}$ eV and above 3.48 $\times 10^{19}$ eV respectively, which indicates a decrease of MC in energy above 9.96 $\times 10^{18}$ eV and also an increase of MC in energies above 3.48 $\times 10^{19}$ eV. In addition, the increasing of

MC at energy above 4×10^{19}eV was reported by the other research group [20] and [21].

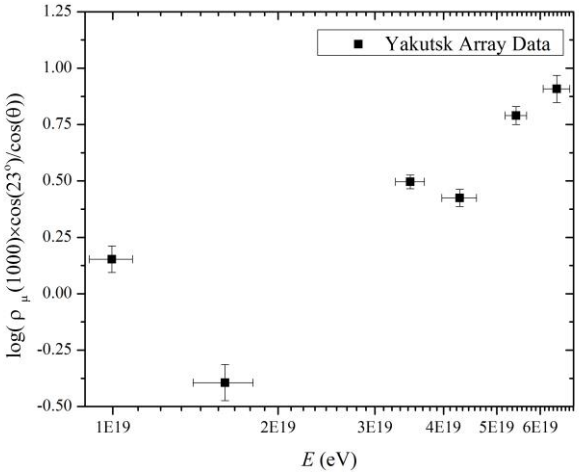

Fig. 8. Muon density variations at distance of 1000 m from the core vs. energy for Yakutsk array data.

3. MC Discrimination

In this session, it is tried to estimate the percentage of MC of elementary CR regarding to some sensitive parameters to MC. As it was mentioned, values of Q, S and β parameters are different for different primary CR mass at the same energy. So, the Q and also β parameter decrease with the increase of particle mass. At the present work, MC of EAS is studied by comparing all of the mentioned parameters, and the results are shown in Table 2.

Table 2

Data and results of MC at present work by using Yakutsk array data.

No.	Shower ID	Zenith Angle	Primary Energy (eV)	Q(600)	Q(2000)	Age Parameter (S)	(LDF) Slope
1	7903230722	9.24	9.96E18	0.588	0.975	2	-2.31
2	7504080374	9.24	3.17E19	0.731	0.995	1.43	-3.41
3	7805240056	9.59	3.08E19	0.738	0.996	1.38	-3.49
4	7802150215	10.26	5.47E19	0.751	0.996	1.35	-3.59
5	8302080209	10.57	3.6E19	0.770	0.997	1.25	-3.78

6	7503130818	19.77	2.19E19	0.746	0.996	1.37	-3.54
7	8510260556	20.44	4.19E19	0.690	0.992	1.62	-3.04
8	8112011090	20.77	1.2E19	0.658	0.988	1.76	-2.79
9	8002100931	21.72	5.94E19	0.656	0.988	1.77	-2.78
10	8403210855	22.028	3.4E19	0.741	0.993	1.39	-3.50
11	7801080347	22.77	3.76E19	0.575	0.971	2.05	-2.23
12	8304270667	23.50	4.28E19	0.625	0.983	1.87	-2.56
13	7703131040	24.63	5.3E19	0.760	0.997	1.29	-3.70
14	8202230827	27.87	8.55E18	0.693	0.992	1.62	-3.07
15	8501171227	30.23	1.1E19	0.748	0.996	1.37	-3.56
16	7601290974	30.79	1.72E19	0.719	0.994	1.51	-3.28
17	8510230970	33.27	6.54E18	0.682	0.991	1.66	-2.98
18	7810061014	37.25	3.18E19	0.724	0.995	1.46	-3.34
19	7312300951	37.81	4.2E19	0.707	0.993	1.57	-3.17
20	7701141069	37.90	1.48E19	0.712	0.994	1.54	-3.22
21	7204070693	40.53	6.26E19	0.829	0.999	0.83	-4.57
22	7503171202	41.66	3.79E19	0.734	0.995	1.42	-3.43
23	8611300643	41.84	1.18E19	0.7133	0.994	1.53	-3.23
24	7801200404	42.60	3.32E19	0.685	0.991	1.66	-2.99
25	741129056	44.92	3.17E19	0.703	0.993	1.58	-3.14
26	7712211125	46.13	6.43E19	0.539	0.960	2.16	-2.02
27	7712130894	47.07	2.55E19	0.684	0.993	1.7	-2.91
28	7802141209	48.24	2.6E19	0.610	0.980	1.94	-2.45
29	7312170709	48.47	9.38E18	0.655	0.987	1.78	-2.76

30	8511030163	48.70	3.82E19	0.670	0.990	1.7	-2.89
31	7506030949	52.19	4.34E19	0.690	0.992	1.6	-3.06
32	7404140775	54.83	4.57E19	0.643	0.988	1.8	-2.69
33	7911070729	55.38	3.81E19	0.763	0.997	1.28	-3.72
34	8006100329	56.70	5.38E19	0.664	0.989	1.7	-2.86
35	8211120420	59.46	3.38E19	0.622	0.982	1.89	-2.53
36	8002011117	59.73	4.28E19	0.638	0.985	1.84	-2.64

Regarding to Table 2. for showers with low value of parameters; Q(600), Q(2000) and β, it's S oppositely has a high value and vice versa. In fact, as it is expected, the sensitive parameter to the MC are in a fare relative compatibility to each other. So with using this compatibility the MC of primary particles, which formed the showers, can be estimated. At this step some limits were used. To evaluate the Gamma fraction in the primary particles these limits are used; $Q > 0.76$, $S < 1.3$ and $\beta < -3.7$. (Regarding to simulated data of Ivanov et.al. [15], they suppose some limits for S and β while at present work by using from more simulated data and also more parameter such as Q(600), we change S, β and Q a little(. According to the recent survey, around 11% of compositions of the particles are based on the lightest element named as gamma and more than half of them are formed by light and medium element and the rest of them are allocated to heavy and ultra-heavy particles.

4. Results

In the present work, MC of elementary CRs with energies above 5×10^{18} eV is studied by using some observable parameters such as Q parameter, s, lateral distribution function slope β parameter, muon component ρ_μ. therefore, two results are obtained. The First result is a decrease in MC in energy range of $(8 - 9)\times10^{18}$ eV, and the second is an increase in MC for energies above GZK cutoff $(3 - 4)\times10^{18}$ eV; these results are in agreement with other groups results such as that of Auger work.

Also, regarding to the observables for mass discrimination of Yakutsk array data, the percentage of gamma rays are estimated 11% which support the recent Auger Observatory results for 10EeV.

R E F E R E N C E S

[1]. *M. Risse, P. Homala, R. Engel and D. Gora*, "Upper limit on the photon fraction in highest-energy cosmic rays from AGASA Data" Phys. Rev. Lett. **vol. 95**, Oct. 2005. 171102.

[2]. *M.D. Healy*, " Composition Sensitive Parameters Measured With The Surface Detector of the Pierre Auger Observatory" in proc. 30th International Cosmic Ray Conference (ICRC) Mexico, **vol. 4**, 2008. p.p 377.

[3]. *M. Settimo, Pierre Auger Collaboration*. "An update on a search for ultra-high energy photons using the Pierre Auger observatory" in proc. 32th International Cosmic Ray Conference (ICRC) Beijing, **vol.2**, 2011. p.p 55.

[4]. *J. Abraham, M. Aglietta, C. Aguirre, et al*, " Upper limit on the Cosmic-Ray photon flux above 10^{19} Ev using the surface director or the Pierre Auger Observatory", Astropatr. Phys, **vol**.**29**, 2008. p.p 243-256.

[5]. *P. Bhattacharjee, G, Sigl*, "Origin and Propagation of Extremely High-energy Cosmic Rays" Phys. Rep., **vol.327(3),** Apr. 2000, p.p 109-247,.

[6]. *G.B. Gelmini, O. E. Kalashev and D. V. Semikoz*," GZK Photons as Ultra-High-Energy Cosmic Rays" J. Exp. Theor. Phys, **vol. 106**, Jun 2008, p.p 1061-1082.

[7]. *K. Greisen*, " End to The Cosmic-Ray Spectrum" Phys. Rev. Lett. **vol. 16**, Apr 1966, P.P 748.

[8]. *G. T. Zatsepin, and V. A Kuz'min*, "The contribution of the upper atmosphere to small effects in the hard component of cosmic rays during chromospheric flares" Journal of Experimental and Theoretical Physics Letters, **vol. 4**, 1966, p.p 78-80.

[9]. *J. Abraham, P. Abreu, M. Aglietta, et al*. "Observation of the suppression of the flux of cosmic rays above 4×10^{19} eV." Phys. Rev. Lett. **vol. 101**, 2008, 061101.

[10]. *F. Salamida, Pierre Auger Collaboration*. "Update on the measurement of the CR energy spectrum above 10^{18} eV" in proc. 32nd International Cosmic Ray Conference (ICRC), Beijing**, vol.2**, 2011, p.p 145,.

[11]. *J. Abraham, P. Abreu, M. Aglietta, et al*, "Upper limit on the cosmic-ray photon fraction at Eev energies from the Pierre Auger Observatory" Astropart. Phys. **vol.31(6)**, Jul 2009, p.p 399-406.

[12]. *N. N. Efimov, T. A. Egorov, D. D. Hrasilnikov, M. I. Pravdin*, "world data center of Yakutsk array catalog" (1988).

[13]. *M. Nagano and A. A. Watson*, "Observation and implication of the UltraHigh-Energy Cosmic Rays", Rev. Mod. Phys. **vol. 72**, Jul 2000, p.p 689.

[14]. *K. Kamata, J. Nishimura*, " The lateral and the angular structure functions of Electron Showers", Prog. Theor. Phys. Supp, **vol. 6**, 1958, p.p 93-155.

[15]. *A. A. Ivanov, M. I. Pravdin, A. V. Sabourov*, " On the shower age related characteristics of cosmic ray cascades in the atmosphere" in proc. 32th International Cosmic Ray Conference (ICRC) Beijing, **vol.2**, 2011, p.p 35.

[16]. *S. Doostmohammadi, and S.J, Fatemi*, " An investigation of mass composition of Ultra-High energy Cosmic Rays with energy above 10^{19} eV via the study of extensive air shower" Serb.Astron. J., **vol. 184**, 2012, p.p 87.

[17]. J. Nishimura and K. Kamata, " On theaccuracy of the moliere function" Prog. Theeor. Phys. **vol.6(2),** 1951, p.p 262-263.

[18]. *K. Greisen*, "Cosmic Ray Shower" Ann. Rev. Nucl. Part. Sci, **vol. 10**, 1960, p.p 63-108.

[19]. *N. Hayashida, K Honda, M. Honda*, et.al. " Muons (> or =1GeV) in large extensive air shower of energies between $10^{16.5}$ eV and $10^{19.5}$ eV observed at Akeno". J. Phys. G: Nucl. Part.Phys, **vol. 21**, 2008, p.p 1101.

[20]. *A. A. Mikhalov, N. N. Efremov, N. S. Gerasimove, et al*, " Estimate of the Mass Compositionof Ultrahigh Energy Cosmic Rays" in proc. 29th International Cosmic Ray Conference (ICRC) Pune, **vol.7**, 2005, p.p 227-230.

[21]. *A. A. Mikhalov*, " Analysis of the Arrival Direction of Ultrahigh Energy Cosmic Rays" in proc. 30th International Cosmic Ray Conference (ICRC) Mexico, **vol. 410**, Jul 2007, P.P 359.